Spring 5-9-2020

Investigatin Actin-Myosin Mechanics to Model Heart Disease Using Fluorescence Microscopy and Optical Trapping

Justin Edward Reynolds
University of Mississippi

Investigating Actin-Myosin Mechanics to Model Heart Disease Using Fluorescence Microscopy and Optical Trapping

By:
Justin Edward Reynolds

A thesis submitted to the faculty of the University of Mississippi in partial fulfillment of the requirements of the Sally McDonnell Barksdale Honors College.

Oxford
May 2020

Approved by:

X _____
Dr. Nikki Reinemann
Advisor

X _____
Dr. Thomas Werfel
Reader

X _____
Dr. Adam Smith
Reader

Acknowledgements

I would like to thank the Biomedical Engineering Department for supporting me throughout my research as well as the UM STEMS REU Program for allowing me to start my thesis research during the summer. Specifically, I would like to thank Dr. Dwight Waddell for advising me throughout my college career, Dr. Nikki Reinemann for advising my thesis project, and Dr. Thomas Werfel and Dr. Adam Smith for being my readers. Also, I would like to thank Dr. Paris and Dr. Ashpole for the use of their equipment and resources as well as Dr. Lang at Vanderbilt University for the use of his Optical Trap and other equipment.

Abstract

Justin Edward Reynolds: Investigating Actin-Myosin Mechanics to Model Heart Disease Using Fluorescence Microscopy and Optical Trapping
(Under the direction of Dr. Nikki Reinemann)

Hypertrophic cardiomyopathy (HCM) is a hereditary disease in which the myocardium becomes hypertrophied, making it more difficult for the heart to pump blood. HCM is commonly caused by a mutation in the β-cardiac myosin II heavy chain. Myosin is a motor protein that facilitates muscle contraction by converting chemical energy from ATP hydrolysis into mechanical work and concomitantly moving along actin filaments. Optical tweezers have been used previously to analyze single myosin biophysical properties; however, myosin does not work as a single unit within the heart. Multiple myosin interacts to displace actin filaments and do not have the same properties as ensembles versus single molecules. We have engineered a more physiologically accurate optical trapping approach using a hierarchical cytoskeleton structure consisting of multiple myosin between two actin filaments that more closely models how myosin behaves within the heart. The model was verified using fluorescent microscopy, and we analyzed the biophysical properties of healthy myosin-actin complexes to lay the foundation for studying diseased models in the future. For the healthy myosin model, we have measured displacement profiles and force generation capacities using optical tweezers. This assay allows us to not only analyze myosin in a more physiologically relevant environment but also to study how multiple myosin interact within cardiac muscle cells.

Table of Contents

Table of Figures

1 Introduction

As of 2017, the leading cause of death in the United States is due to heart disease[1]. While most cardiac arrest deaths are in older adults, a rare group involves sudden cardiac death in individuals under 35 years of age – especially in adolescent athletes [2]. Many times, these deaths occur with no warning, and are often due to unknown heart defects or overlooked heart abnormalities[2]. A leading cause of sudden cardiac death in adolescent athletes is hypertrophic cardiomyopathy (HCM).

HCM is a hereditary disease that is caused by gene mutations in the heart muscle[3–5]. A common site for these mutations to occur is in the β-cardiac myosin heavy chains[5]. Myosin is a molecular motor protein important for driving muscle contraction. These myosin mutations affect the myocardium, or muscular tissue of the heart, and causes the ventricular septum, the wall between the left and right ventricle in the heart, to grow abnormally thick (Figure 1)[4]. The hypertrophy, or enlargement of the tissue due to the cell size increasing, in the myocardium makes it harder for the heart to pump blood, which can lead to complications such as atrial fibrillation, sudden cardiac death, obstructed blood flow, dilated cardiomyopathy, mitral valve problems, or heart failure[2,4]. Many individuals with HCM show minimal to no symptoms, but their condition could be exposed during exercise[3,4]. Due to many individuals appearing asymptomatic, it commonly goes undiagnosed in patients and is one of the leading underlying causes for sudden cardiac death while exerting oneself[3,4]. While HCM outcomes have been studied in asymptomatic patients, the molecular basis of the disease is not yet well understood[3–5]. Studying HCM from a molecular level will allow the scientific community to better understand how the

molecular motor's mechanical function differs between a normal cardiac muscle and the mutated system seen in hypertrophic cardiomyopathy[6].

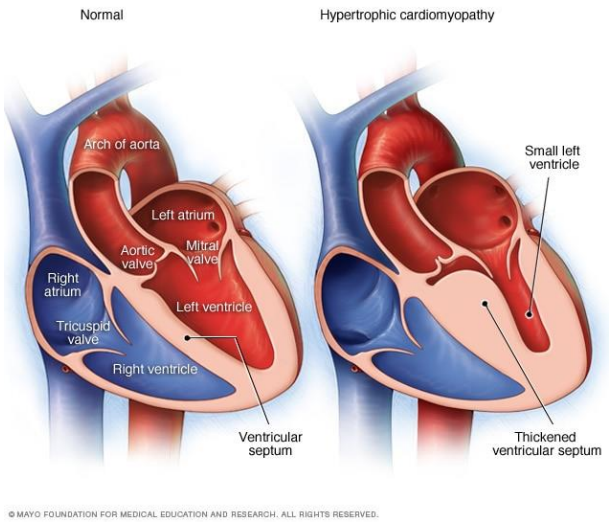

Figure 1 Hypertrophic Cardiomyopathy (Illustrations of a normal heart (left) and a heart with hypertrophic cardiomyopathy (HCM). Note that the heart walls (muscle) are much thicker (hypertrophied) in the HCM heart.)[4]

Molecular motors are vital to living organisms. They are the proteins that transform chemical energy into mechanical work through ATP hydrolysis[7,8]. In doing so, they translocate cellular filaments, such as microtubules and actin, to perform large scale tasks, such as controlling cell movement and division[6,8]. There are three types of molecular motors, but for this study, cardiac myosin II is analyzed.

In order to better understand how the heart functions when healthy and in a diseased state, we developed a novel assay that is more physiologically relevant than previous single molecule studies of myosin to analyze the molecular basis of heart muscle contraction[6]. Myosin's force generating performance was measured using optical trapping and fluorescence microscopy techniques[9,10]. Optical trapping allows for the measurement of very precise mechanics of protein systems, with nanometer displacement and piconewton

force resolution[6,11]. Previous studies have been conducted using optical trapping, but those studies have only analyzed myosin as a single unit acting on a single actin filament[6,12]. However, we know that this is not an accurate representation of the actin-myosin complex *in vivo*. In cardiac muscle cells, multiple actin and myosin work together to cause heart contractions. To mimic this function, we have engineered a more physiologically relevant model of the actin-myosin complex. The new assay allows us to measure the molecular-level mechanics of actin-myosin systems important for heart muscle contractions. The capabilities measured will allow us to better understand the disease and give insight to the molecular consequences of HCM.

The study of this hierarchical and more physiologically relevant model (see more in Methods) will allow the scientific community to gain insight to the mechanical differences between a normal actin-myosin complex compared to the mutated system. The resolution of optical trapping will allow for the mechanics of molecular motor ensembles to be studied more in depth and precisely than previously. Understanding the system from a molecular level could reveal a pathway to exploit for therapeutic intervention and better screen patients for this condition.

2 Background

2.1 Cardiac Muscle Function

Cardiac muscle tissue is a specialized form of muscle tissue that is responsible for pumping blood to the entire body[13]. It is made up of many interlocking muscle fibers, and each fiber is striated, containing a single nucleus. Cardiac muscle cells have evolved to have high contractile strength and endurance[14]. It maintains its own rhythm and has the ability to spread electrochemical signals that cause contraction in unison[14–16]. The striation of the fiber can be used to see where the different components are, such as actin and myosin. As seen in Figure 2, the dark bands are areas of thick protein filaments made up of myosin (see more in Myosin), while the light bands are thin filaments made up of primarily actin (see more in Actin). During muscle contractions, the myosin pulls the actin filaments together causing the contractions[13,14]. The sinoatrial node (SA node) regulates when the heart contracts (Figure 3). It is the heart's natural pacemaker. The SA node causes the action potential that leads to contraction. The signals from the SA node travel through the internodal pathways to the atrioventricular node (AV node) down the bundle of His, the fibers that deliver the electrical signal to the left and right ventricle, leading to activation of the left and right ventricle. The potential is terminated in the Purkinje fibers[14,16]. The cells are able to function in this way because they form a giant network of cardiac muscle cells through their connection by their intercalated disks (Figure 4). The intercalated disks form tight junctions between the cells holding them together while under strain and allowing electrochemical signals to be passed quickly. This connection leads to the wave-like contraction pattern seen by the heart's electrocardiogram[13,14].

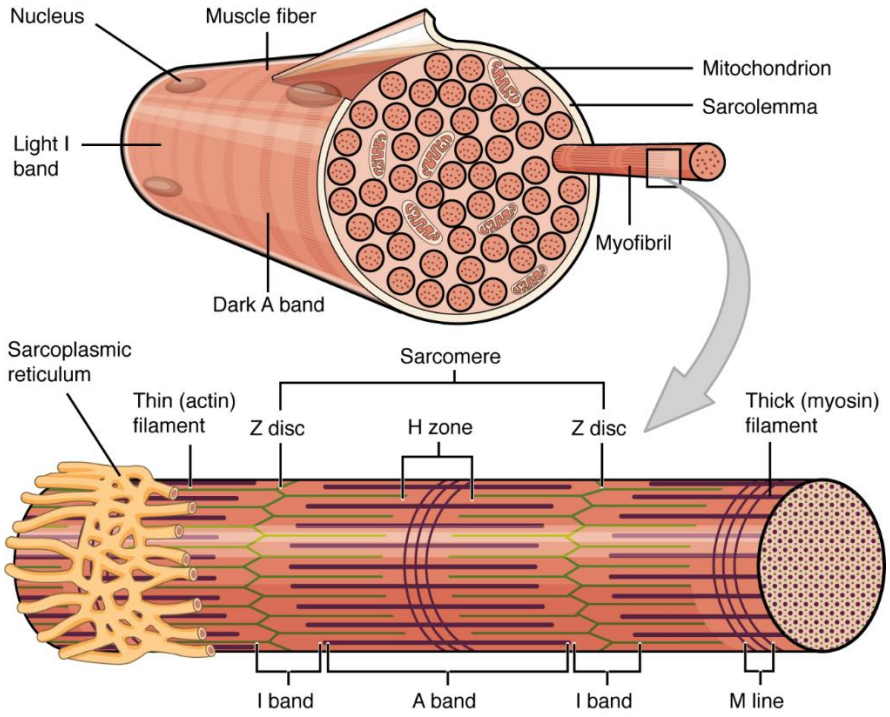

Figure 2 Histology of Muscle[17]

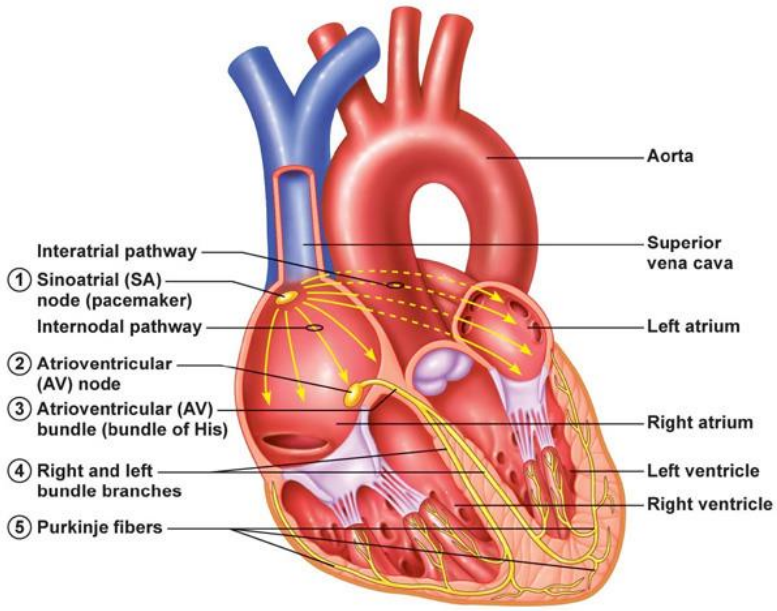

Figure 3 Electrical Signals of the Heart[18]

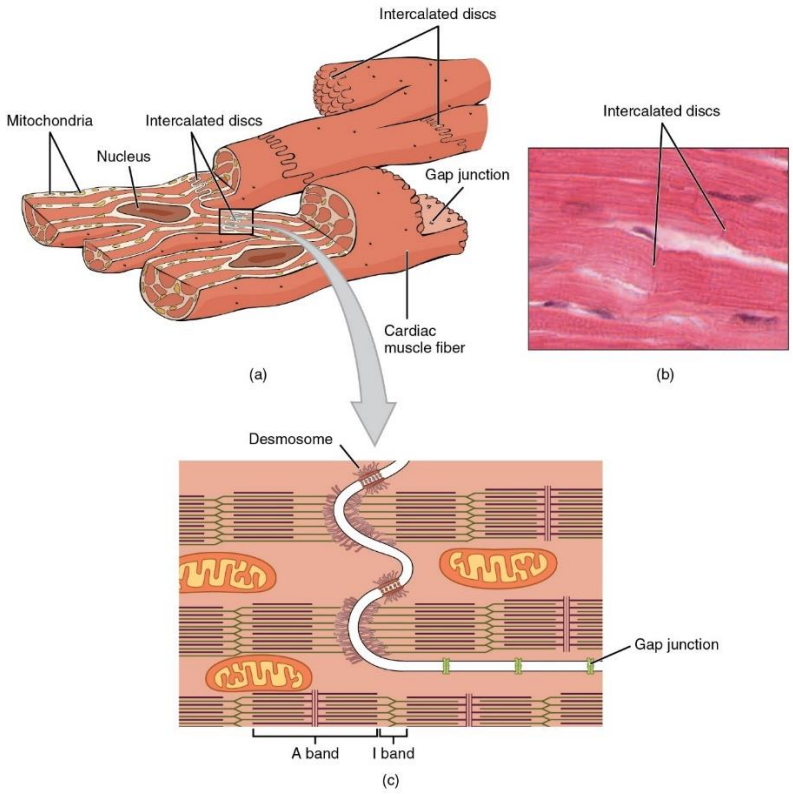

Figure 4 Cardiac Muscle and Electrical Activity[15]

2.2 Actin

Cardiac muscle contractions are conducted by two proteins – actin and myosin (see more in Myosin). The myosin's motor head pulls the actin filament causing it contract like an accordion, and this leads to the muscle contractions in the heart (see more in Actin-Myosin Complex). Actin is the major cytoskeletal protein for most cells and is the thinnest, ~7 nm in diameter, of the three principal types of filaments[19]. Actin filaments are abundant in the cell and help provide mechanical support, determine cell shape, allow movement of the cell surface, and act as a track for molecular motor movement[12,19]. It enables cells to perform functions such as migration, engulfing particles, and dividing[19]. Globular, monomeric actin proteins polymerize to form actin filaments, and these filaments are organized into higher-order structures, forming bundles or three-dimensional networks,

within the cell[19]. Their assembly and disassembly, crosslinking into bundles, and association with other cell structures are regulated by a variety of actin-binding proteins. Actin filaments add and lose subunits only at their ends[20,21]. This is done through a process called treadmilling. Treadmilling is a phenomenon observed in cytoskeletal filaments, and it occurs when one end of a filament grows in length while the other end shrinks leading to the seeming "moving" of the filament (Figure 5)[8,19,20]. The process of treadmilling, or actin polymerization, requires ATP, and the subunits incorporate into the filament once ATP hydrolyzes into ADP[19,20]. Treadmilling occurs because actin are structurally polar, but not in the sense of electrostatics[8]. Polarity refers to the speed of polymerization and growth of the filament. The "plus" or barbed end is the faster polymerizing end, and the "minus" or pointed end is slower polymerizing. This structural polarity is important for directionality of protein transport[19,21].

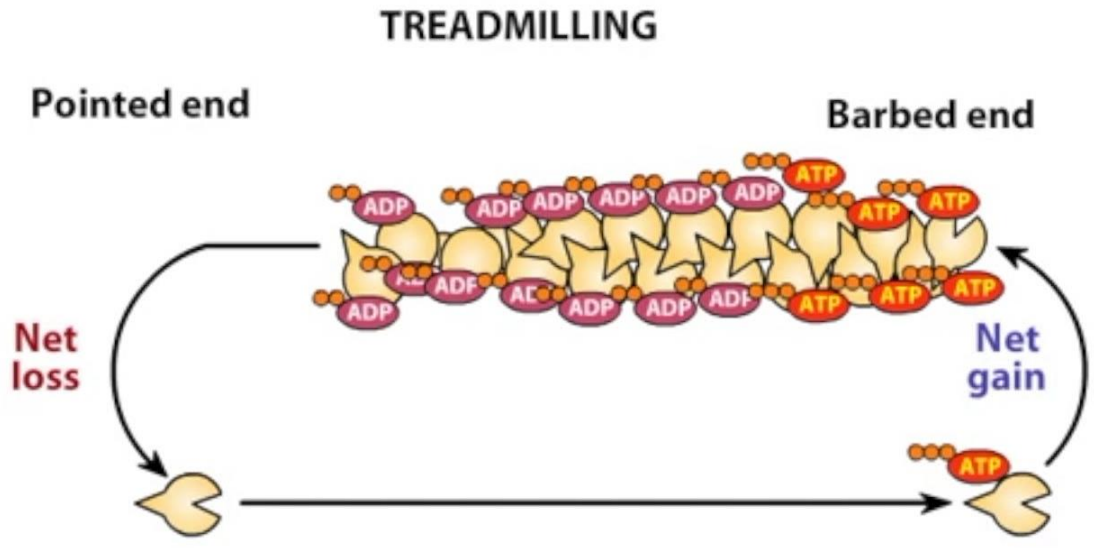

Figure 5 Actin Treadmilling Process[22]

2.3 Myosin

Myosin is another protein that plays a role in cardiac muscle contractions. Myosin, a mechanoenzyme, is a molecular motor protein that converts chemical energy into mechanical work[7,12,23]. They do this to transport and anchor organelles, vesicles, and other intracellular components. Myosin are the only known actin-based motor protein and are a large and diverse superfamily made up of many different classes[8,23,24]. In our study, we are focused on the muscle myosin II family, which are responsible for muscle contraction in skeletal as well as cardiac muscle through the ATPase cycle. The first myosin II was discovered in 1864 by Willy Kuhne. Myosin II have long α-helical tails and two heavy chains with globular heads that have binding domains that are used to produce the "power stroke" (see more in Actin-Myosin Complex) in the actin-myosin complex (Figure 6)[23,24]. Myosin II aggregates to form thick filaments (Figure 6b) that interact with actin in the cross-bridge cycle (Figure 7)[8,17]. The filaments are formed by the interaction of the α-helical tail domains in an antiparallel orientation[23,24].

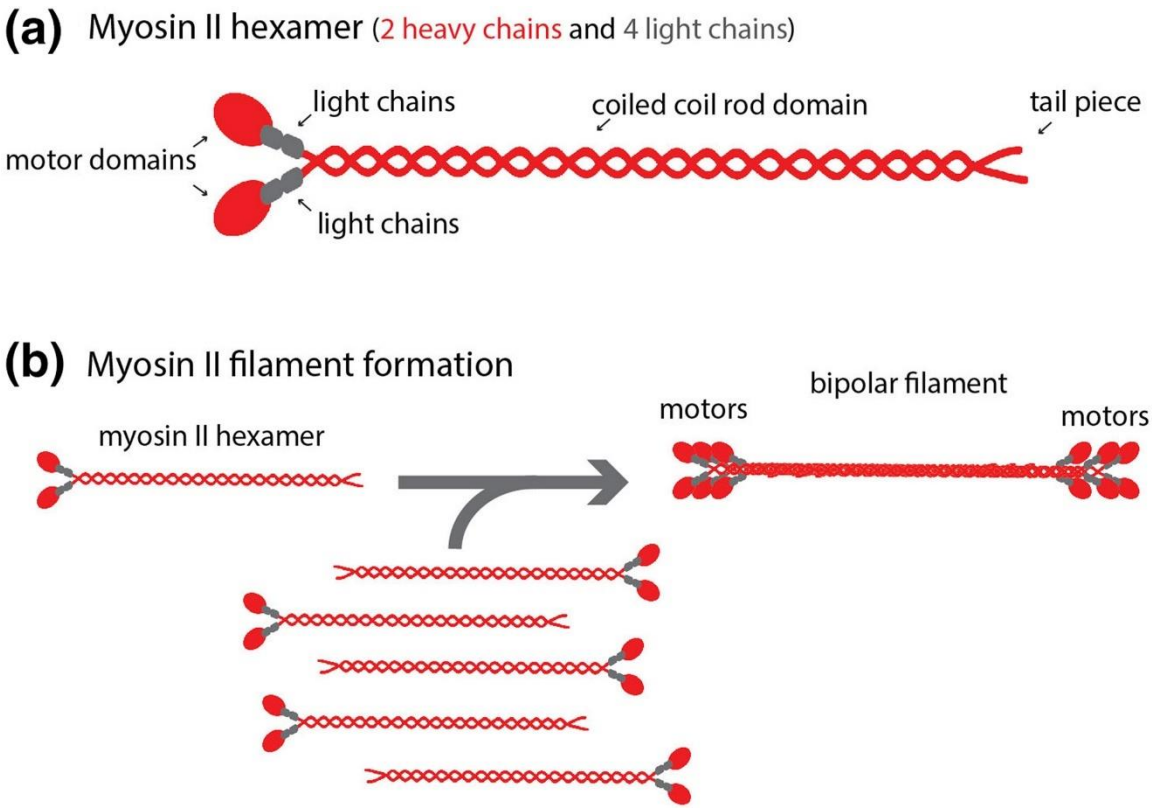

Figure 6 Myosin II Structure & Assembly[24]

2.4 Actin-Myosin Complex

The actin-myosin complex is responsible for muscle contraction through the hydrolysis of ATP in the actin-myosin cross-bridge cycle[8,12]. The contractile elements are in highly organized arrays the give the characterization patterns of cross-striations – such as the light and dark bands in muscle fibers[13,17]. The sliding filament model is the currently accepted model for muscle contractions, which was proposed in 1954 by Andrew Huxley, Ralph Niedergerke, Hugh Huxley, and Jean Hanson[25]. During the muscle contraction, each sarcomere, the contractile unit of the muscle cell composed of interacting myosin and actin filaments, shortens similarly to an accordion[25,26]. The cross-bridge cycle begins with the myosin head in its high energy conformation with ADP and P_i attached. The release of P_i

forms the cross-bridge with the myosin head cocking and binding to the actin filament. Then, ADP is released and causing the power stroke and the contraction of the actin filament. At this point, myosin is in its low energy conformation. ATP then binds to the myosin head and releases it from the actin filament. ATP is hydrolyzed into ADP and $P_{i,}$ and the process restarts itself (Figure 7)[8,25].

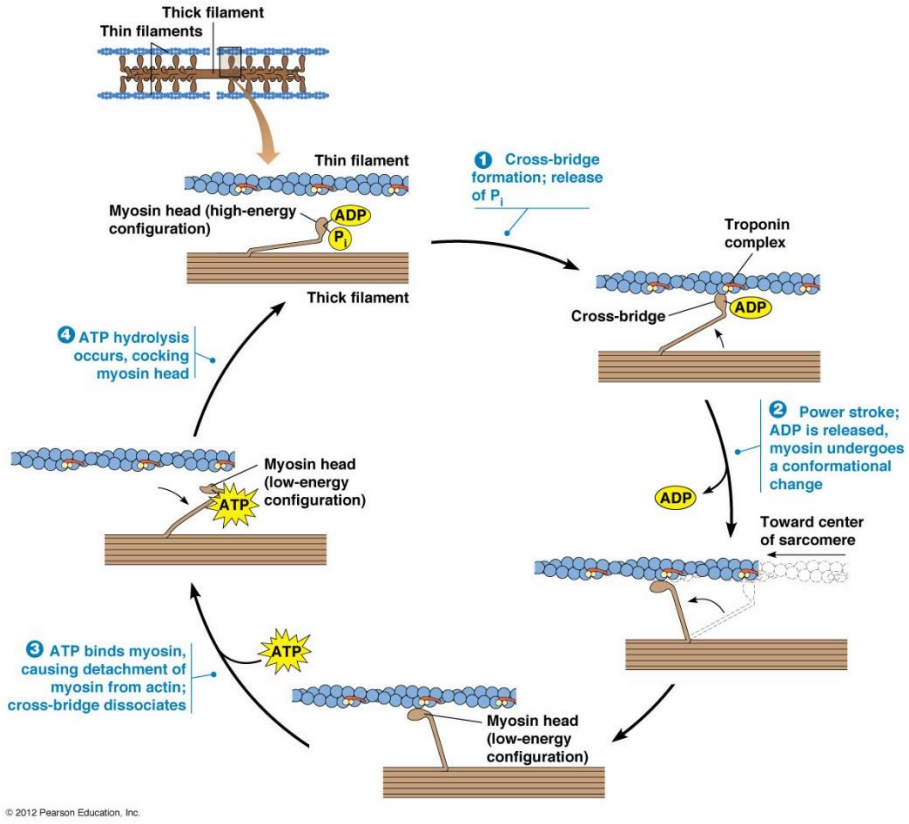

Figure 7 Actin-Myosin Cross-Bridge Cycle[25]

2.5 Optical Trapping

In our study, we used a biophysical technique called optical trapping to study the biophysical properties of the actin-myosin complex[6,27]. The optical trap (optical tweezers) was developed by Arthur Ashkin, and he was awarded the Nobel Prize in Physics in 2018 for his work[28]. Optical tweezers are able to use light to manipulate microscopic objects as

small as 10 nm using the radiation pressure from a focused laser beam[29]. This instrument is able to accurately measure distance and force down to a nanometer and piconewton range, which allows for the mechanical properties of biological motors to be analyzed [29]. The trap functions because light has momentum[10]. When a highly focused laser beam with a gaussian profile is passed through a glass or polystyrene bead, that bead experiences a gradient force that pushed the bead to the center of the trap where the light intensity is the highest (Figure 8)[10,29]. Since the photons focused around the bead are trapping it in the center of the gaussian laser, the force generated by the molecular motor of interest can be found by relating the distance the molecular motor pulls the bead from the center of the trap to the force produced by using Hooke's Law (see more in Theoretical Principles, Figure 9).

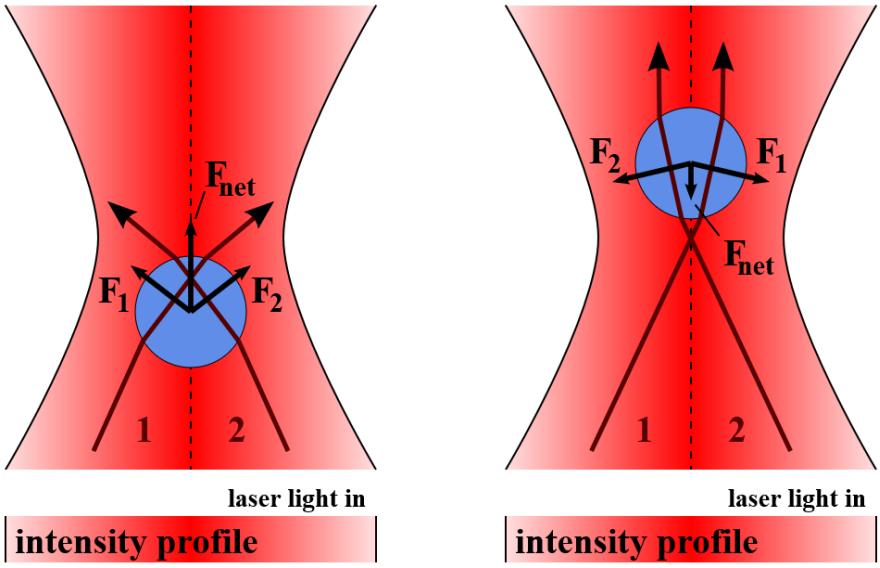

Figure 8 Gradient Force (left image net force up towards the center of the trap laser; right image net force down towards the center of the trap laser)[30]

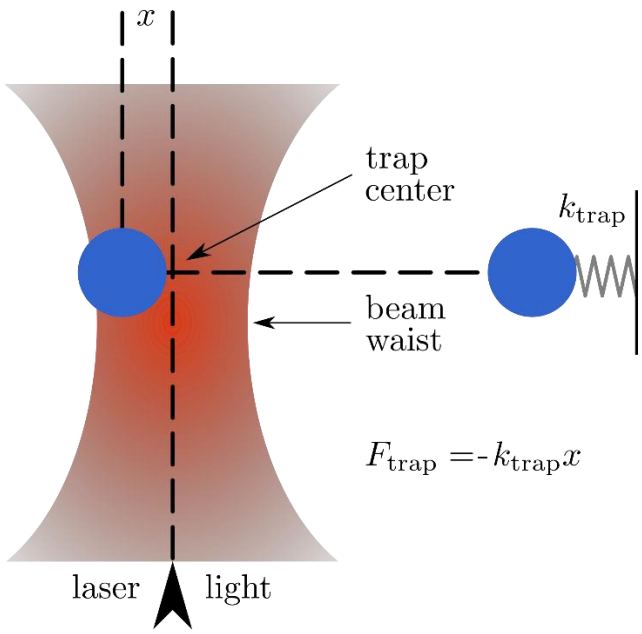

Figure 9 Hooke's Law (Relates displacement to force of the attached molecular motor.)[30]

Optical trapping is a useful tool in our study because the force and position resolution are on the same scale as molecular motor properties, such as force generation capability, motor head step size, and velocity[6,10,11]. Here, we were mainly concerned with the force generation capabilities of myosin, force mechanics of motor-filament assemblies, as well as their displacement as single motors and as an ensemble. Optical tweezers are able to analyze these molecular ensembles that are made up of multiple motors and actin filaments, or an actin-myosin complex or "bundle". Being able to analyze the force generation capability and motor head step size of the "bundle" will help to gain insight to understanding the molecular basis of hypertrophic cardiomyopathy[6,12,27,31].

2.6 Fluorescence

Fluorescent microscopy is a technique used in this study to visualize the molecular-level components of our assays. Fluorescence can be performed using a microscope with an intense light source, such as an arc lamp or laser, and fluorophores or dyes in the

sample[9]. This tool is especially useful for biology because it provides high contrast of the sample, has a high specificity, is a quantitative measure, and allows for live cell imaging[32]. Fluorophores or a dye are added to stain the sample and create a better contrast between structures[9]. Once the fluorophores or dyes are added and the sample is stained, light, usually in the visible or ultraviolet (UV) range, is used to excite the fluorophores, causing the emission of a lower energy light from the sample. This process causes changes in electron energy states, as seen in a Jablonski diagram (Figure 10) [32–35]. As the excitation photons hit the sample, the sample's electrons are forced to a higher energy state. Then, the electron loses energy and returns to an intermediate ground state. As the electron returns to the ground state, it releases photons at a lower energy and longer wavelength than the excitation light, giving the emission spectrum.

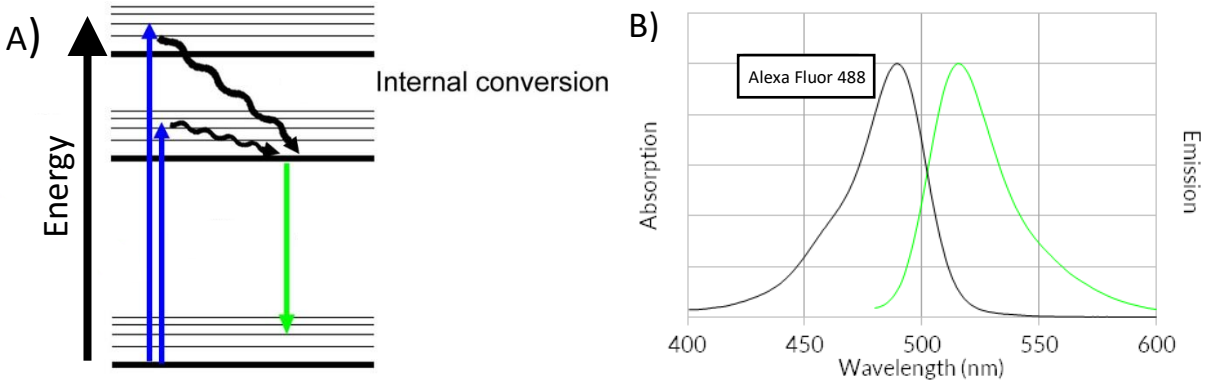

Figure 10 (A) Jablonski Diagram (B) Alexa Fluor 488 Excitation/Emission Spectrum (A: Alexa Fluor 488 Jablonski Diagram; B: Alexa Fluor 488 Excitation/Emission Spectrum)[35,36]

In our study, we used two dyes – rhodamine and Alexa 488. Rhodamine and Alexa 488 have a similarity in their structure as they both have a lot of conjugation[37,38]. Conjugation refers to the double bonds that can be seen in Figures 11 and 12. These structural properties of the molecule give rise to each dye's unique characteristics[39]. This is due to the equation for photon energy (see more in Theoretical Principles)[40]. Energy and

wavelength have an inverse relationship, and as conjugation increases, the energy barrier decreases due to electron delocalization. Since conjugation and wavelength have a linear relationship, as the conjugation of a structure increases, wavelength also increases. It is the extent of conjugation that helps create these specific color properties[33,39]. For example, when using rhodamine, the dye is excited with green, ~532nm, and it emits the longer wavelength and lower energy red[37]. Another example is when using Alexa Fluor 488, the dye is excited with blue, ~488nm, and it emits the lower energy of green[38,41]. The benefit of fluorescence in our study is that it allowed us to visualize individual assay components and verify that actin-myosin bundles formed properly. As shown in a later section, by staining the bottom layer of actin with rhodamine and the top layer with Alexa Fluor 488, we were able to use fluorescence microscopy and the program ImageJ to verify that the sandwiched bundles were binding together properly (see more in Methods)[6,37,38,42,43].

Photobleaching, the photochemical alteration of a dye or fluorophore causing it to lose its fluorescence, can occur with fluorescent microscopy if the sample is continuously exposed to the excitation light. In the case of photobleaching, measures can be taken, such as adding an oxygen scavenging unit, to preserve the life of the dyes (See Methods).

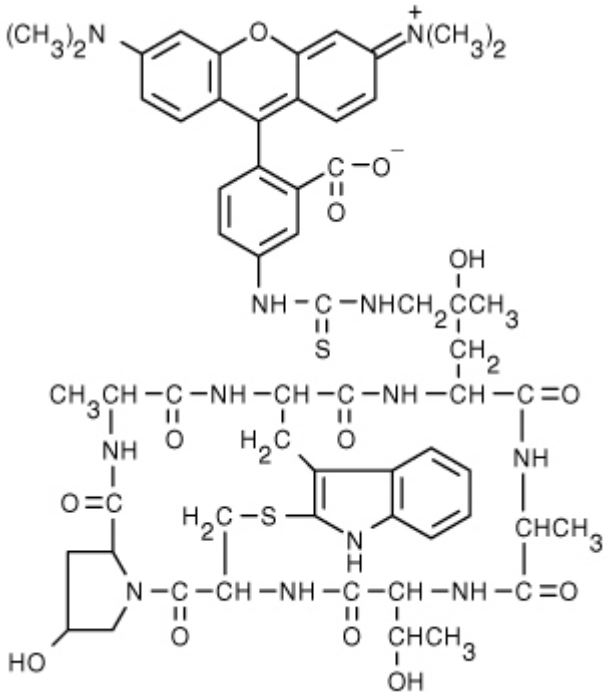

Figure 11 Rhodamine Phalloidin Structure[37]

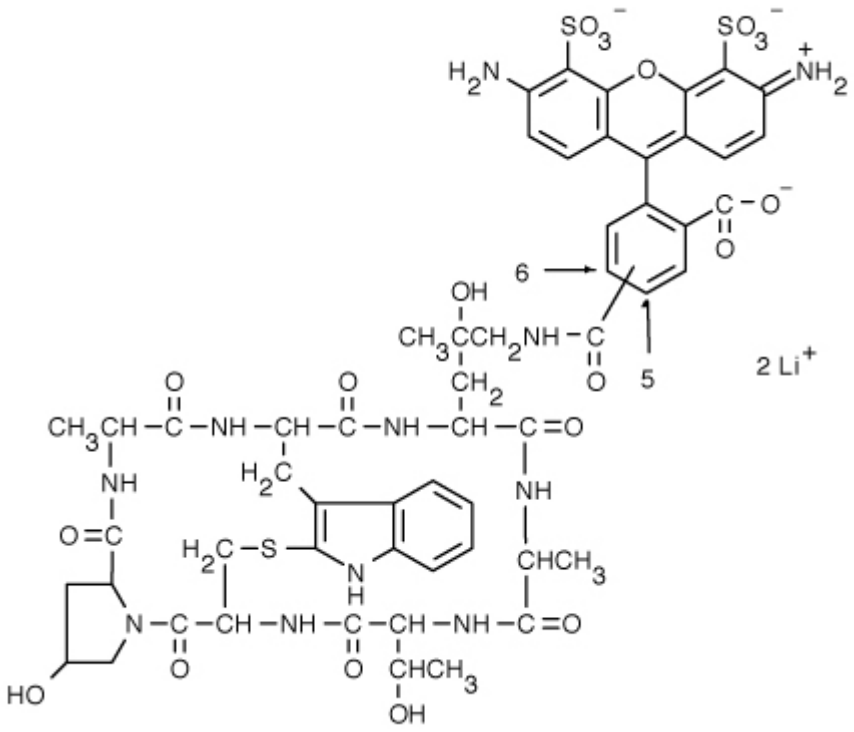

Figure 12 Alexa Fluor 488 Phalloidin Structure[38,41]

2.7 Previous Studies

To date, myosin and actin have not been studied as molecular ensembles in a hierarchical, physiologically relevant context using optical tweezers. The only previous work performed involves single molecule studies, which is not accurate to physiology *in vivo*. However, these single molecule studies were helpful in identifying properties of individual myosin motors and in developing a protocol for our model. An important study was one of Ashkin's first optical trapping papers where optical trapping of dielectric particles by a single-beam gradient force trap was demonstrated for the first time[27]. These and many other studies that have been conducted have allowed us to see the potential of optical trapping as a tool in our study, but the most notable previous work was the three-bead trapping assay of Finer *et al.*[6,7,11,12,16,29,31,44].

The article "Single myosin molecule mechanics: piconewton forces and nanometre steps" was an influential single molecule study to our current work. James Spudich's group was able to use optical trapping techniques to measure myosin mechanics at the single molecule in the piconewton and nanometer range[6,11]. They used a three-bead assay in their study that consisted of two trapped beads with actin attached to each[6,27]. The third bead was stuck to the microscope slide and had myosin attached to it[6]. Measurements were taken as the myosin motor contracted the actin filaments due to hydrolyzing ATP (Figure 13)[6,24]. The results of this study showed that the average displacement, "step size", of each myosin power stroke was 11nm and the myosin produce an average force of 3-4 pN per power stroke[6,15,26]. The results in this article build a strong foundation for studying myosin using optical trapping by identifying and characterizing essential motor properties. In addition, by having the single molecule properties of myosin moving on actin, we can use that

information to deduce mechanisms of how multiple myosin motors work together within the complexes in our study[6,7,27,31].

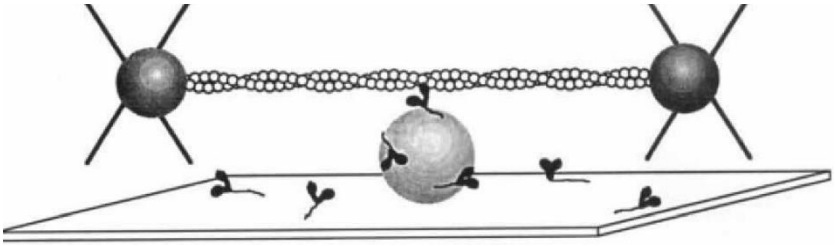

Figure 13 Three-Bead Assay (Finer et al.)[6]

2.8 Motivation for Current Study

HCM in patients has been studied at various levels, but the molecular basis of the disease is still not well understood[3,4]. Therefore, we used a technique traditionally used for single molecule experiments (optical trapping) to study the properties of assembled actin-myosin bundle complexes *in vitro*[8,15]. Optical trapping allows the mechanical work of myosin molecular motors to be measured with nanometer displacements and piconewton force resolution, while fluorescent microscopy techniques will allow for the novel bundle assay to be visualized[6,27,32,33]. Previous studies show the need to make model assays that can be engineered to study the mechanical work exerted by myosin II in a more realistic environment[6,31]. Studying the mechanical properties of a more physiologically relevant model of cardiac muscle cells will lead the scientific community to a better understanding of the molecular basis of HCM.

3 Methods

3.1 Etching Coverslips

Etching microscope coverslips is an important cleaning step to make sure that there are no contaminates remaining on the slide from the company. It also promotes a better binding environment of the proteins onto the slide's surface.

3.1.1 Cleaning Coverslips Protocol

1. Dissolve 100 g of KOH in 300 mL of ethanol in a beaker. Stir with a stir bar until KOH is dissolved.
2. Put coverslips in Teflon racks.
3. Fill one beaker with 300 mL of ethanol and two more beakers with 300 mL of reverse osmosis H_2O. Degas all four beakers (KOH in ethanol, ethanol, two beakers with water) for 5 minutes in the bath sonicator on the degas setting.
4. Submerge the rack of coverslips in the beaker with the KOH, an sonicate for 5 minutes.
5. Dip the rack of coverslips up and down in the beaker with ethanol until ethanol runs off the coverslips smoothly (no beading).
6. Dip the rack of coverslips up and down in the beaker of water until the water runs off the coverslips smoothly (no beading).
7. Submerge the rack of coverslips in the other beaker of water and sonicate for 5 minutes.
8. Spritz with water until the water flows off the coverslips smoothly.
9. Spritz with ethanol until the ethanol flows off the coverslips smoothly.
10. Dry the rack on the over for about 15-20 minutes.

3.2 Solution and Buffers

The solutions and buffers used in our study play an important role in making sure that the integrity of the proteins is maintained. It is important to make sure that the proteins do not denature. Solution T, TC Buffer, FC Buffer, GAB, APB, and PBS, and are all used to keep the proteins in their optimal pH range. Without the correct pH range, the proteins will denature and no longer function.

3.2.1 Solution T Protocol

1. In a 50 mL Falcon tube, add:
    a. 3.940 g Tris-HCl
    b. 0.147 g $CaCl_2$
2. Add reverse osmosis water to 50 mL total volume and mix well. (500 mM Tris-HCl and 20 mM $CaCl_2$
3. Label Solution T and store at 4˚C.

3.2.2 TC Buffer Protocol

1. Add 40 mL of reverse osmosis water and 1.5 mL of Solution T to a 50 mL Falcon tube. Mix well.
2. Adjust the pH to 8.0 by adding small volumes of concentrated KOH. (Usually 4-5 pellets of KOH to a 50 mL Falcon tube, fill with deionized water, and use this to adjust pH)
3. Add water to a final volume of 50 mL and verify the pH. Adjust pH if necessary.
4. Label the tube TC and store at 4˚C.

3.2.3 FC Buffer Protocol

1. Mix:
    a. 85 mL of reverse osmosis water
    b. 10 mL of Solution T
    c. 3.728 g KCl
    d. 0.0406 g $MgCl_2$
2. Adjust the pH to 7.5 by adding small volumes of concentrated KOH.
3. Add water to a final volume of 100 mL and verify the pH. Adjust pH if necessary.
4. Label the tube FC and store at 4˚C.

3.2.4 General Actin Buffer (GAB) Protocol

1. Mix:
    a. 485 µL of TC buffer
    b. 10 µL of 10 mM ATP
    c. 5 µL of 50 mM DTT
2. Label as GAB and store at 4˚C.

3.2.5 Actin Polymerization Buffer (APB) Protocol

1. Mix:
    a. 455 µL of FC buffer
    b. 25 µL of 100 mM ATP
    c. 20 µL of 50 mM DTT
2. Label as APB and store at 4˚C.

3.2.6 1x PBS Protocol

1. Add 24.73 g of 10x PBS powder to 250 mL buffer bottle.

2. Add reverse osmosis water to 250 mL total volume. Mix well.
3. Verify pH is 7.4. Adjust if necessary.
4. Need to dilute 10 times to get to 1x PBS.
5. Add 10 mL of 10x PBS and 90 mL of reverse osmosis water to a 100 mL buffer battle. Mix well. Verify pH. Store at 4˚C

3.3 Actin Preparation

Two actin types are polymerized for each assay. We use unlabeled actin and biotinylated actin. The biotinylated actin is important for our attachment to our streptavidin coated beads (see more in Bundle Assembly). The biotin/streptavidin interaction is used extensively in the optical trapping field due to it being one of the strongest noncovalent interactions, their availability, and ease of use in trapping assays. The reconstituted actin will be stained with rhodamine phalloidin while the reconstituted biotinylated actin will be stained with Alexa Fluor 488 phalloidin. Phalloidin is a toxin that binds actin between polymerized subunits and stabilizes actin filaments. By staining the polymerized actin two different colors, we are able to verify that the bundle assay has properly formed and adhered to the flow cell (see more in Flow Cell Assembly).

3.3.1 Polymerizing and Staining Actin Filaments Protocol

1. Reconstitute Actin by adding 100 μL of reverse osmosis water to 1 mg vial of lyophilized actin. Mix well by pipetting up and down. Aliquot into 5 μL samples. Store at -80˚C.
2. Thaw one vial of 10 mg/mL pure actin.
3. Prepare fresh GAB.

4. Add 50 μL GAB and mix well by gently pipetting up and down. Place on ice for 1 hour.
5. Prepare fresh APB.
6. Polymerize actin by adding 5.5 μL of APB to the actin solution. Mix well by pipetting up and down in a gentle fashion. Place on ice for 20 minutes.
7. Add 5 μL rhodamine phalloidin (stains and stabilizes the actin filaments). Leave on ice in the dark for 1 hour.
8. Store in the dark at 4˚C. Stable for about 1 week.

3.3.2 Polymerizing and Staining Biotinylated Actin Filaments Protocol

1. Reconstitute Actin by adding 100 μL of reverse osmosis water to 1 mg vial of lyophilized actin. Mix well by pipetting up and down. Aliquot into 5 μL samples. Store at -80˚C.
2. Reconstitute biotinylated actin by adding 20 μL of reverse osmosis water. Aliquot 5 μL samples. Store at -80˚C.
3. Thaw one vial of 10 mg/mL pure actin and 1 vial of 1 mg/mL biotinylated actin.
4. Prepare fresh GAB.
5. Add 100 μL GAB and mix well by gently pipetting gup and down. Place on ice for 1 hour.
6. Prepare fresh APB.
7. Polymerize actin by adding 11 μL of APB to the actin solution. Mix well by pipetting up and down in a gentle fashion. Place on ice for 20 minutes.

8. Add 5 μL Alexa Fluor 488 phalloidin (stains and stabilizes the actin filaments). Leave on ice in the dark for 1 hour.
9. Store in the dark at 4˚C. Stable for about 1 week.

3.4 Myosin and Bead Preparation

Myosin from Cytoskeleton, Inc. is supplied as a lyophilized powder and must be reconstituted into the correct concentration. Beads from Spherotech need to be cleaned once they arrive to make sure no residual contaminates are on them. The beads come already coated in streptavidin. Streptavidin has a high binding affinity for biotin and allows for our bead to bind to the actin biotinylated actin filaments (see more in Bundle Assembly).

3.4.1 Reconstitute Myosin II Protocol

1. Briefly centrifuge to collect the product at the bottom of the tube.
2. Reconstitute to 10 mg/mL by the addition of 100 μL of reverse osmosis water containing 1 mM DTT
    a. 1 mM DTT in reverse osmosis water
        i. 0.01542 g in 1 mL reverse osmosis water
    b. Add 100 μL of 1 mM DTT to the tube
    c. The protein will be in the following buffer: 25 mM PIPES, pH 7, 1.25 M KCl, 2.5% w/v sucrose and 0.5% w/v dextran.
3. Dilute stock myosin 10x by adding 10 μL of stock myosin to 90 μL of 1 mM DTT in reverse osmosis water.
4. Make 3 μL aliquots. Snap freeze aliquots in liquid nitrogen.
5. Store at -80˚C.

3.4.2 Wash Streptavidin-Coated Beads Protocol

1. Dilute 20 µL 0.44 µm streptavidin-coated beads into 80 µL PBS.
2. Wash 4 times at 10,000 rpm for 6 minutes, reconstituting in 100 µL PBS.
3. Sonicate for 2 minutes at 40%.
4. Store washed beads on a rotator at 4˚C.

3.5 Flow Cell Assembly

The flow cell creates a channel that we can wash our reagents through to assemble the bundle assay (see more in Bundle Assembly).

3.5.1 Constructing a Flow Cell Protocol

1. Combine 30 mL of ethanol with 200 µL of poly-l-lysine.
2. Soak an etched coverslip in the poly-l-lysine (promotes protein binding to the glass coverslip) mixture for 15 minutes.
3. Take a microscope slide and apply two strips of double stick tape a few millimeters apart.

4. Break off the excess tape.

5. Carefully place the poly-l-lysine soaked coverslip on top perpendicular to the microscope slide.

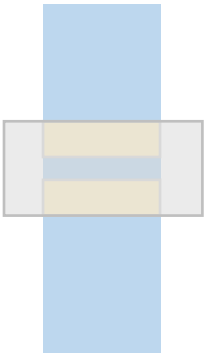

6. Use an epp tube to gently press against the coverslip to ensure the flow cell is properly stuck together.

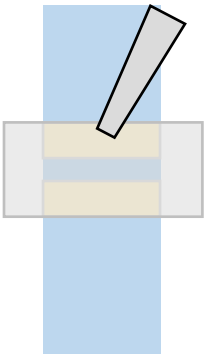

7. Flip flow cell over so that the coverslip is on the bottom. Flow cell channel should hold 10-20 µL of liquid.

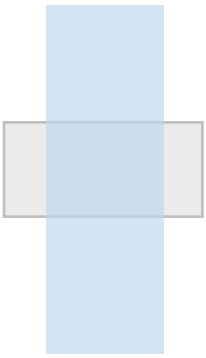

8. Use pipets to add solutions slowly. Use Kim wipes to slowly wick the solution through without causing the flow cell to dry out.

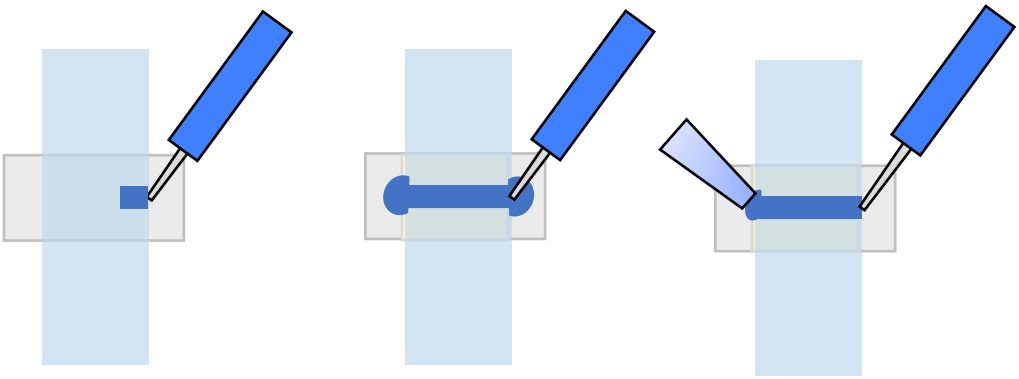

Figure 14 Flow Cell Assembly

3.6 Oxygen Scavenging System

The oxygen scavenging system allows for the fluorescent actin to be viewed without photobleaching too quickly. The system extends the life of the fluorescent dyes and allows for enough time to verify the bundle before the fluorescence gets too dim.

3.6.1 Oxygen Scavenging System Protocol

1. Glucose oxidase
    a. 25 mg/mL in PBS.
    b. Aliquot into 5 µL samples.
    c. Store at -80˚C

2. Beta-D-glucose
    a. 500 mg/mL in PBS
    b. Aliquot into 5 μL samples.
    c. Store at -80˚C.
3. Catalase
    a. Dilute 500 μL into 500 μL PBS.
    b. Aliquot into 5 μL samples.
    c. Store at -80˚C.
4. Combine 1 μL each of glucose oxidase, beta-D-glucose, and catalase when using fluorescent dyes.

3.7 Bundle Assembly

The “bundle” is the novel model of the actin-myosin complex that we have engineered to analyze the mechanical properties of myosin II. The bundle consists of rhodamine stained actin bound to the coverslip with myosin II sandwiched between the rhodamine stained actin and the Alexa Fluor 488 biotinylated actin. The Alexa Fluor 488 biotinylated actin is bound to a streptavidin coated bead (Figure 15).

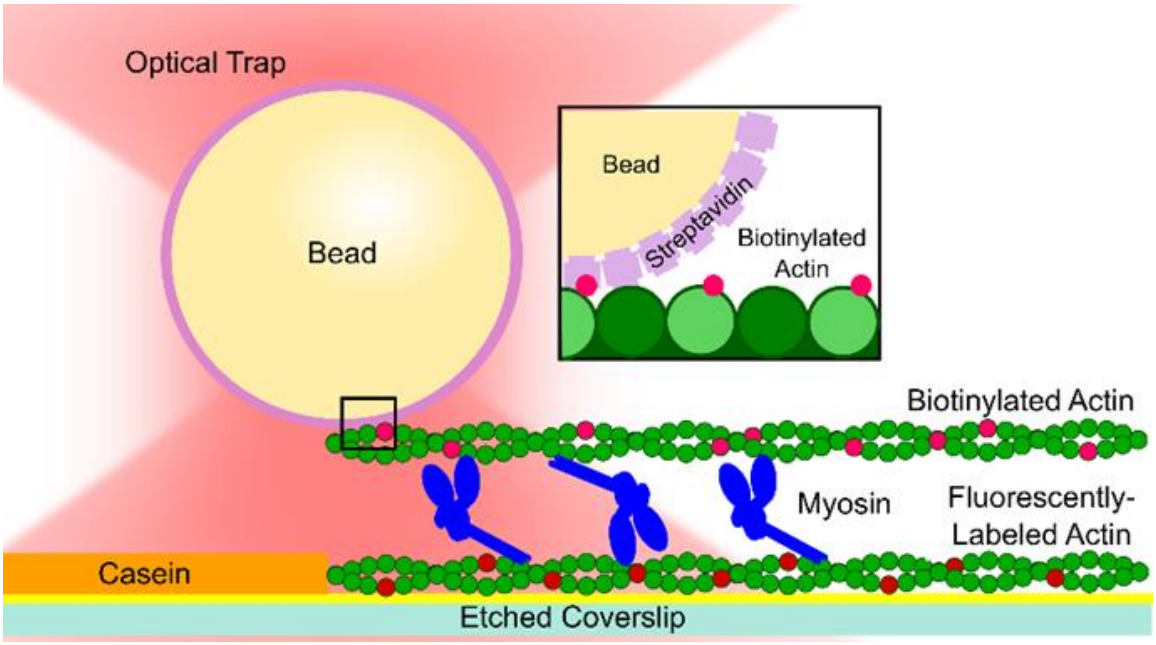

Figure 15 Desired Bundle Assay

3.7.1 Bundle Assembly Protocol

1. Dilute the Alexa Fluor 488 biotinylated actin 500x in GAB.
2. Combine 15 µL of Alexa Fluor 488 biotinylated actin, 1 µL of diluted and cleaned streptavidin beads, 1 µL of 100 mM ATP, and the oxygen scavenging system. Put in the rotator and let sit while the bundle is assembled.
3. Dilute the rhodamine actin 500x in GAB.
4. Add 15 µL of the 500x dilute rhodamine actin to the flow cell. Let incubate for 10 minutes in humidity chamber.
5. Wash flow cell with 10 µL of GAB. Pull through with a Kim wipe.
6. Dilute casein 10x in GAB = 1 mg/mL casein.
7. Add 10 µL of 1 mg/mL casein (blocks binding to the glass coverslip and ensures that only rhodamine actin is bound to the glass) to the flow cell. Let incubate for 5 minutes in humidity chamber.

8. Add 1 μL of 1 M myosin to combination in the rotator from step 2.
9. Add the combination from step 8 to the flow cell. Pull through with a Kim wipe.
10. Seal the channel of the flow cell with nail polish so it does not dry out.

3.8 Optical Trap Operation

The optical trap is a complex instrument that has specific protocols for set-up, use, obtaining data, and analysis. The optical trap we use can be seen in Figure 16. When the trap was delivered, one of the company's representatives came to train all of us on the device. The following protocol is used to load flow cells and get them into focus on the optical trap.

Figure 16 Optical Trapping Set-Up

3.8.1 Setting up the Optical Trap Protocol

1. Turn on the control box and the trapping laser.
2. Start the JPK optical trap computer software.
3. Turn on the laser to 50 mM, and let it stabilize for 30 minutes.
4. Remove the sample holder from the trap's microscope stage.
5. The objectives are water immersion based. Add 30 μL of reverse osmosis water onto the bottom objective
6. Load the flow cell coverslip down onto the stage and reinserted into the trap.
7. Raise the lower objective until the bead of water touches the coverslip.
8. Add 170 μL of reverse osmosis water to the top of the slide.
9. Lower the top objective until it breaks the surface tension of the water.
10. Begin to get the tape on the slide in focus using the bottom objective.
11. Once the tape is in focus, switch from bright field to DIC, and close the iris.
12. Bring the top objective down until you see an octagonal shape. This is to get the objectives in Koehler illumination. Get the edges of the shape as sharp as possible. Reopen the iris, switch back to bright field, and lock to two objectives (only lets them move as one unit).
13. Find a bead floating in solution. Trap it by clicking the trap shutter button, which will open the shutter to allow the trapping laser to hit the sample. Once trapped, the bead needs to be calibrated so that voltage measurements can be correlated to force and displacement.
14. Run the calibration routine within the software for the X, Y, and Z directions. Make sure to "accept values" for each.

15. Release the bead, and find a bundle by searching for beads stuck to actin filaments. Filaments can be visualized in DIC if they are thick enough or in fluorescence mode.
16. Verify that a bundle is present by looking for both fluorescent actin filaments. Turn the filter cube to 532 nm to verify the presence of the rhodamine filament in the bundle, and then turn the filter cube to 488 nm to verify the presence of the 488 filaments.
17. Once verified, trap the bead attached to the top filament of the bundle by unshuttering the trapping laser (click the button).
18. Click the "record data/live oscilloscope" button to record data. Choose which data you wish to visualize (position, force, x direction, y direction), click autosave, and click record.
19. Data will be saved as .out files. These can be exported into Excel, separated into columns by space, and you can then analyze the recorded force and displacement data versus time.

3.9 Analyzing Data

The data was obtained using fluorescent microscopy and optical trapping techniques. Initial bundles were verified using Dr. Ashpole's fluorescence microscope in Pharmacy and subsequently viewed using ImageJ. ImageJ allowed us to verify that the two actin filaments are truly bound. We checked these two different ways. First, we analyzed our fluorescent images and compared the pixel to see if actin filaments were bound directly on top of each other. Second, we combined the rhodamine and Alexa Fluor 488 channels and saw a yellow actin filament for any bundle that was on the image. The "step size" and

force measurements were analyzed in Excel, and the graphs were made using Igor Pro (see more in Results).

4 Theoretical Principles

4.1 Fluorescence Microscopy and Dyes

The basic principles behind fluorescece dye excitation and emission can be explained by a Jablonski diagram (see Fluorescence section) and the equation for energy of a photon[9,33,40]. The energy of a photon is inversely proportional to the wavelength, so as the energy barrier decreases the wavelength must increase[40]. This is why we see a dye such as rhodamine get excited with green, a shorter wavelength, and emit red, a longer, lower energy wavelength[9,37].

4.1.1 Energy of a Photon

$$E = \frac{hc}{\lambda}$$

Where E is the energy of a photon, h is Planck's constant, c is the speed of light in a vacuum, and λ is the wavelength of a photon[40].

4.2 Optical Trapping

The force acting on a bead in an optical trap acts similarly to a spring, so we can use Hooke's Law to find the force exerted by myosin II[6,27,45]. Trap calibration plays an integral role in taking accurate data[29,31,34]. Once the trap is calibrated, the force can be calculated using Hooke's Law[45]. The calibration step uses the known energy of the laser to find the trap stiffness (k_{trap}; how tightly the bead is held in the center of the trap)[29]. Once the trap stiffness is known, the optical trap will record the displacement of the bead from the center of the laser. Knowing the trap stiffness and the displacement of the bead allows for the calculation of the force that was exerted by the molecular motor[6,11,45].

There are three main calibration methods, and the optical trap we use is calibrated using the power spectrum method. The power spectrum method is a calibration method

that utilized the natural fluctuation in Brownian motion of the bead trapped in fluid to find the stiffness of the trap[29,46]. The calibration method assumes that the system is linear and in a harmonic potential. A harmonic oscillatory system is one that experiences a restoring force proportional to the displacement when displaced from its equilibrium position[47]. For the power spectrum method in an ideal system, we know the temperature of the fluid on the slide and the Boltzmann constant, so we can calculate the stiffness of the trap by watching the displacement of the bead due to Brownian motion. However, the calculation is not that simple because the bead will fluctuate differently based on the different frequencies that interact with the bead. Since the bead will have a spectrum of fluctuation, the power spectrum corrects for this. The spectral density, or bead displacement within the laser trap, will be plotted, and the trap stiffness can be determined from the corner frequency, which is a boundary in a system's frequency response at which energy flowing through the system begins to be reduced rather than passing through (Figure 17)[46,48]. By measuring the power spectrum, we are able to calculate the corner frequency allowing us to find the trap stiffness since we know the drag force for the bead[46].

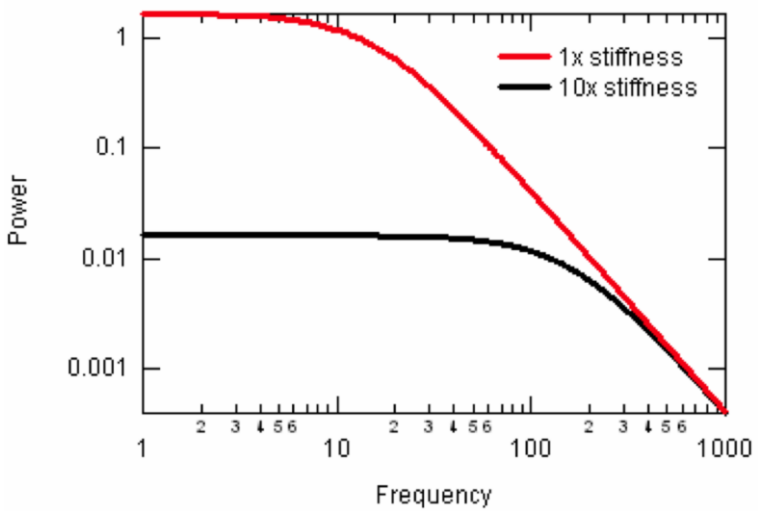

Figure 17 Power Spectrum Method (Example of a corner frequency)[29]

4.2.1 Hooke's Law Derivation

Definition of the potential energy stored in a spring:

$$U = \frac{1}{2}k(x - x_0)^2 \quad (1)$$

Where U is the potential energy stored in a spring, K is the spring constant, x is the change in length, and x_0 is the equilibrium length. Assuming:

$$x_0 = 0;\ x_i = x;\ x_f = x + dx \quad (2)$$

Where dr is a very small change in length. Now looking at the change in potential energy:

$$dU = U_f - U_i \quad (3)$$

Plugging in (2) to (3), we get:

$$dU = \frac{1}{2}k(x - x_0)^2 - \frac{1}{2}kx^2 \quad (4)$$

Expanding (4), we get:

$$dU = \frac{1}{2}k(x^2 + 2xdx + dx^2) - \frac{1}{2}kx^2 \quad (5)$$

Simplifying (5), we get:

$$dU = kxdx + \frac{1}{2}kdx^2 \quad (6)$$

If dx << 1, $dx^2 \rightarrow 0$ and we get:

$$dU = kxdx \quad (7)$$

Now looking at the conservation of energy equation:

$$dE = dK + dU = 0 \quad (8)$$

Where K is the kinetic energy and E is the mechanical energy. Setting (8) equal to zero, we get:

$$dK + kxdx = 0 \quad (9)$$

Rearranging (9), we get:

$$dK = -kxdx \quad (10)$$

Now looking at the work-energy theorem:

$$dK = \vec{F} \cdot d\vec{x} \quad (11)$$

Where $\vec{F}$ is the force vector and $d\vec{x}$ is the displacement vector. Assuming the force vector and displacement vector are going in the same direction, we see:

$$\vec{F} \cdot d\vec{x} = Fdxcos\theta; cos\theta \rightarrow 1 \quad (12)$$

Simplifying (12), we get:

$$\vec{F} \cdot d\vec{x} = Fdx \quad (13)$$

Combining (10), (11), and (13), we get Hooke's Law:

$$F_{trap} = -k_{trap}x \quad (14)^{49}$$

4.2.2 Equipartition and Power Spectrum Method Derivation

Brownian motion of the trapped bead is equal to $\frac{1}{2}k_BT$, whereas the potential energy of a spring is equal to $\frac{1}{2} \propto x^2$. The equipartition method of calibration is accomplished by setting these two energies equal and solving for the stiffness:

$$\propto = \frac{(x^2)}{k_B T} \quad (1)$$

Where $\propto$ is the spring stiffness, x is the displacement of the bead, k_B is the Boltzmann constant, and T is the temperature of the liquid medium. Now, measuring the frequency spectrum of the Brownian noise exhibited by the bead, the mass of the bead is typically so small that the Reynolds number is very low and inertial forces are much weaker than those of hydrodynamic drag. This leads to the equation of motion for the bead being that of a massless, damped oscillator driven by Brownian motion:

$$\beta \dot{x}(t) + \alpha x(t) = F(t) \quad (2)$$

Where x is the position of the bead, $\beta = 6\pi\eta r$ is the drag coefficient of the bead, η is the viscosity of the surrounding fluid, and r is the bead radius. The Brownian noise source, F(t) has zero mean, and essentially white with amplitude:

$$\left|\tilde{F}(f)\right|^2 = 4\beta k_B T \quad (3)$$

Where β is the drag coefficient of the bead, k_B is the Boltzmann constant, and T is the temperature. Taking the Fourier transform, $\tilde{F}(f)$; $\tilde{x}(f)$, of (3) gives:

$$2\pi\beta\left(\frac{\alpha}{2\pi\beta} - if\right)\tilde{x}(f) = \tilde{F}(f) \quad (4)$$

Where i is the imaginary unit. Therefore, the power spectrum is then given by:

$$|\tilde{x}(f)|^2 = \frac{k_B T}{\pi^2 \beta\left[\left(\frac{\alpha}{2\pi\beta}\right)^2 + f^2\right]} \quad (5)$$

Equation (5) is that of a Lorentzian with corner frequency $f_c = \frac{\alpha}{2\pi\beta}$, so the stiffness of the trap is then given by $\alpha = 2\pi\beta f_c$. This method must be repeated for the x, y, and z direction[29,46].

5 Results and Discussion

5.1 Developing a Protocol

Since we had to develop this new and novel cytoskeletal model, an important part of our study was to verify and build a protocol to assemble the actin-myosin bundle assay. We hypothesized that if we promoted binding by soaking the coverslip in poly-l-lysine to promote binding, we could then push actin through the flow cell and it will bind to the surface of the coverslip. Poly-l-lysine is able promote binding because it is positively charged while actin has many negative charges on its surface. Then, excess actin will be flushed out by washing the flow cell with GAB. We do not want our subsequent proteins and actin filaments to bind to the positively charged surface; we want everything else to bind to the prebound actin filaments. Therefore, we block the binding to the surface by pushing casein, a common blocking protein, through the flow cell. Now that surface binding is blocked, we can push biotinylated actin, myosin, and ADP (putting myosin in its strongest binding conformation; ATP would be subsequently added in to the actual assay to facilitate force generation) into the flow cell causing myosin to bind and sandwich between the two actin filaments. Before we begin assembling the bundle, we had to make sure that the actin concentration allowed the visualization of single actin filaments. We started by polymerizing and staining actin filament to make sure that we were able to visualize the actin filaments. Once the actin filaments were polymerized and stained, we viewed them under the fluorescent microscope. Our initial protocol was successful but too concentrated to effectively build bundles; so, we tried dilutions until we found that the 500x dilute actin gave us enough space between actin filaments to allow for the measurement of a single bundle assay (Figure 18). Now that we are able to get the actin

filaments into a working concentration, we can begin assembling the bundle assay and tweak the concentrations of the bundle protocol.

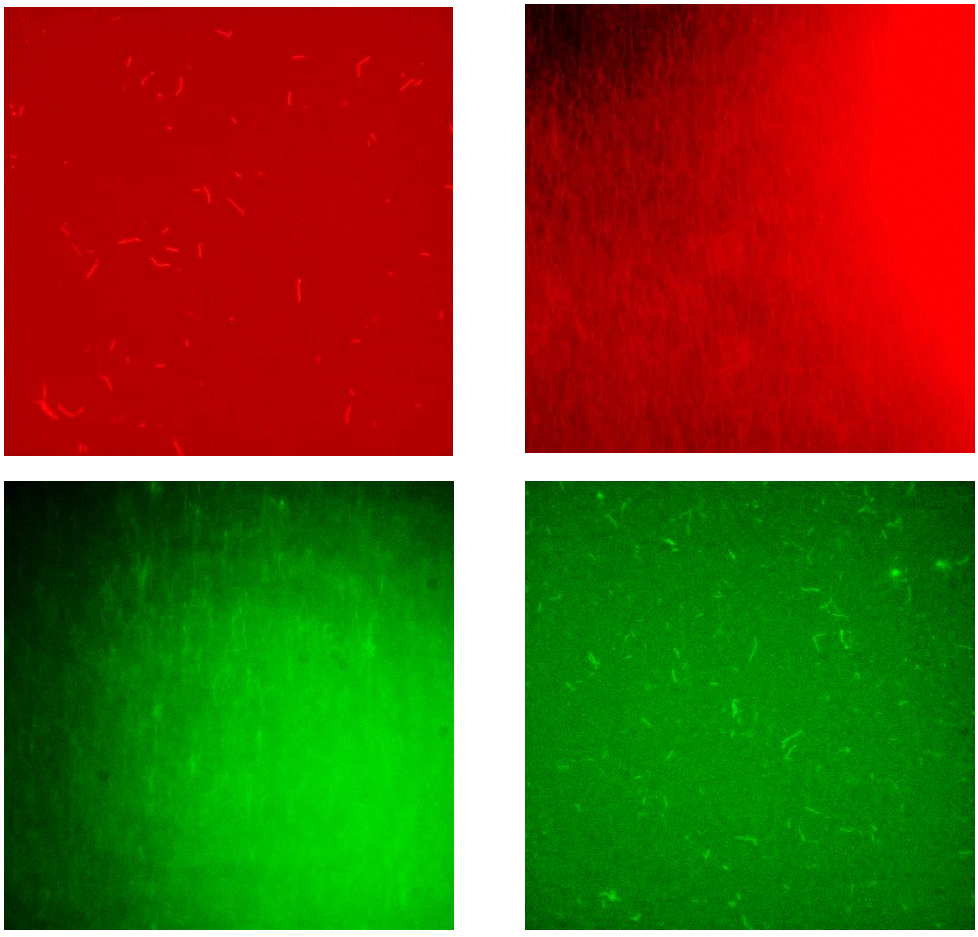

Figure 18 Fluorescent Actin Filaments (Top left: 500x dilute rhodamine actin; Top right: concentrated rhodamine actin; Bottom left: concentrated Alexa Fluor 488 actin; Bottom right: 500x dilute Alexa Fluor 488 actin)

5.2 Verifying the Bundle Assay

To verify the bundle assay was created, we continued to use fluorescent microscopy techniques. Since we stained our actin with two different dyes, we were able to put the flow cell with the bundles into a fluorescent microscope and take pictures of the same frame in both the rhodamine and Alexa Fluor 488 channels. Once the images were taken, we were

able to analyze them using ImageJ and compare each pixel on the side by side frames to see if any bundles were formed and perfectly lined up with one another, which would verify that binding had occurred (Figure 19). Although we verified that the bundle assays were forming correctly, we saw that the actin filaments were breaking apart while we were viewing them on the microscope. This led us to believe that the concentration of myosin II was too high compared to the concentration of actin used, and the force and conformations of the myosin were causing the actin filaments to break. After adjusting the myosin concentration, we saw stable bundle assays that were spaced far enough apart from each other that they could be analyzed; so, we moved into the next phase of our study and began taking preliminary force data of the bundle assay.

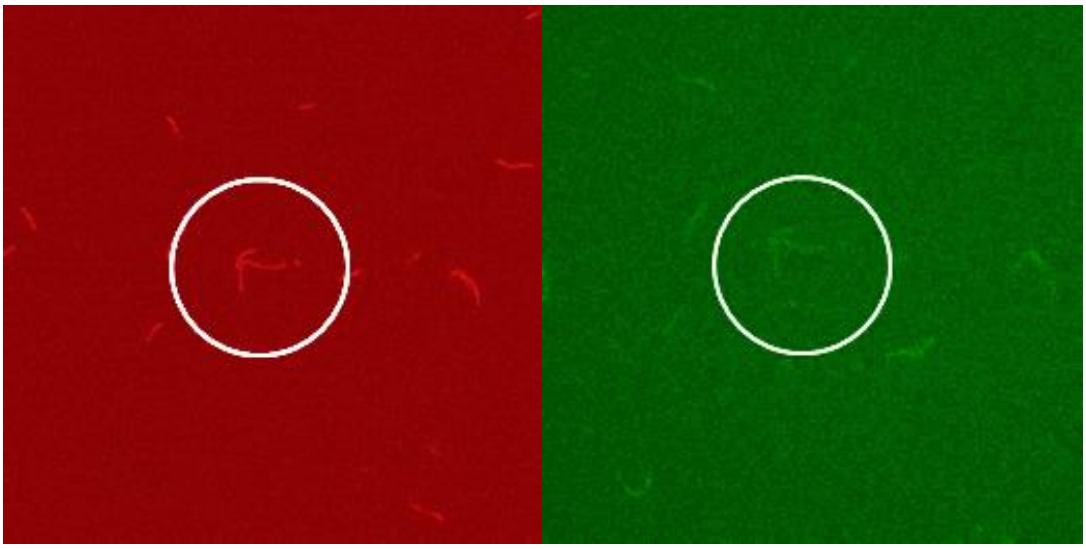

Figure 19 Bundle Assay Formation Verification

5.3 Preliminary Measurements

Now that bundle assay formation is verified, we began taking force generation data of the actin-myosin complex with optical tweezers. First, we trapped an unbound bead in solution and used this bead to calibrate the optical tweezers. We then analyzed the results

of the unbound bead as a control (Figure 20). The unbound bead should produce no data other than Brownian motion – the natural random movement of a particle in solution due to molecules colliding. As seen in Figure 20, the unbound bead showed almost no change in displacement or force and oscillated at baseline. The control measurement verified that the trap was calibrated, and we could begin analyzing the bundle assays. We identified a bundle assay with a streptavidin bead attached to the Alexa Fluor 488 biotinylated actin and trapped the streptavidin bead using the optical tweezers. We were able to obtain multiple traces from multiple bundles on each flow cell that we made. After analyzing the data, we observed that myosin II at the concentration used produced a logarithmic growth pattern (Figure 21-22). In Figure 21 and 22, we can see that the position/force vs. time graph staircases up to a maximum output. The preliminary results of this study showed that in our novel model of the actin-myosin complex, myosin II was able to produce a force between 0.5-3 pN and an average force of 1.3 pN. The myosin II "step size" had more variability but ranged between 5-8 nm on average.

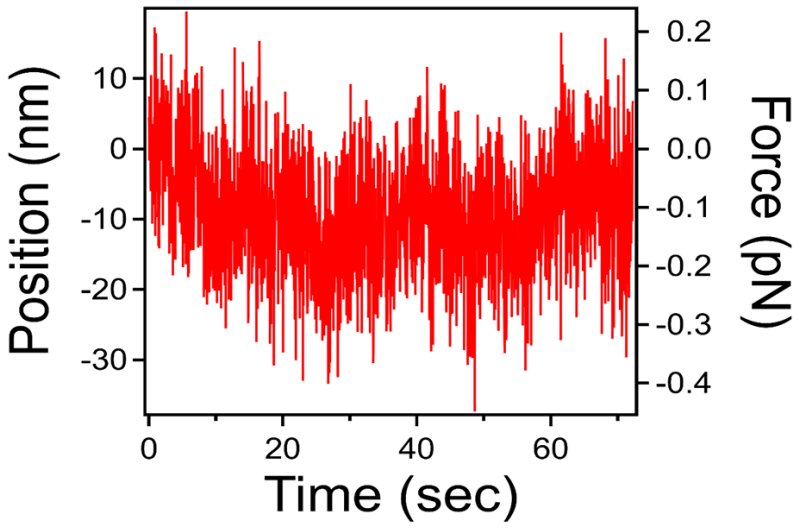

Figure 20 Control Trap Measurement (Bead trapped in solution)

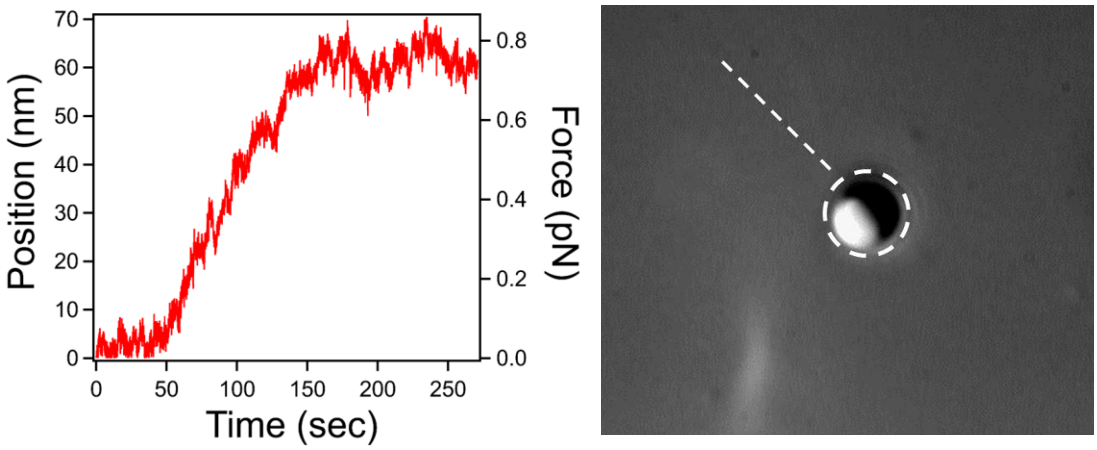

Figure 21 Representative Bundle Trap Measurement 1 (Left: bead trapped and attached to a bundle assay; Right: image of the bead and the highlighted bundle it is attached to)

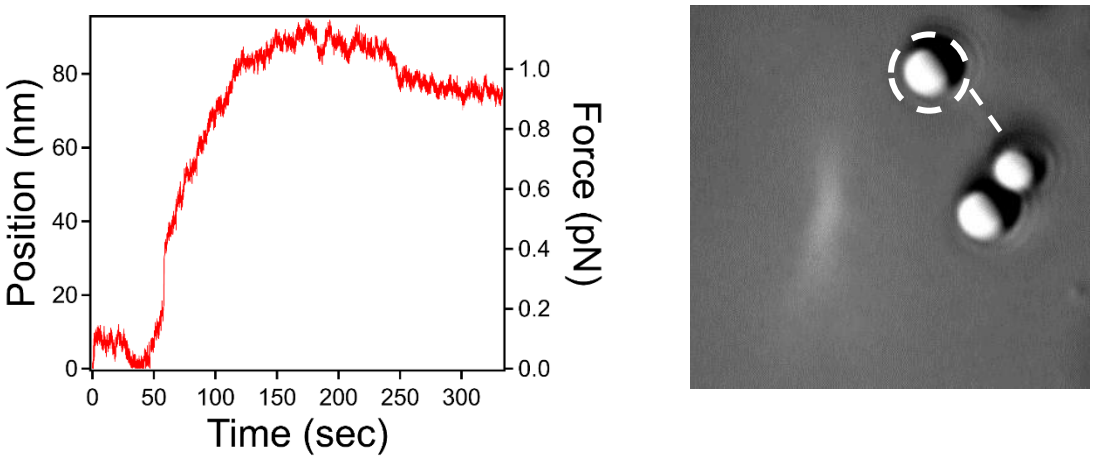

Figure 22 Representative Bundle Trap Measurement 2 (Left: bead trapped and attached to a bundle assay; Right: image of the bead and the highlighted bundle it is attached to)

6 Conclusions and Future Work

The work conducted thus far validates the hypothesis that a new and novel model of the actin-myosin complex could be engineered, and fluorescent microscopy and optical trapping techniques could be used to analyze myosin II's biophysical properties. Our results showed that the "step size" varied and had an average range of 5-8 nm, which was conclusive with myosin studies[6,12]. The interesting difference seen was in the force output of the myosin. Our results showed an average for of 1.3 pN, which was less than the 3-4 pN force outputs seen in previous single myosin molecule studies[6,12]. We hypothesize that the average force in the multiple myosin and actin system is due to competing forces acting in opposite directions causing an antagonizing motion and net force generation that is less. These preliminary studies were the first experiments performed in the Reinemann lab, so there are not any hard conclusions yet from this study. However, it helped confirmed our lab's hypothesis, developed and optimized the protocols for this study, and built a foundation on which we can continue to study this project. Looking forward, the Reinemann Lab Group will continue analyzing healthy myosin models and begin to analyze models with diseased myosin to see if the diseased myosin model's biophysical properties differ from the normal (control) myosin model. Continuing to study the mechanical properties of this more physiologically relevant model of cardiac muscle cells will lead the scientific community to a better understanding of the molecular basis of hypertrophic cardiomyopathy.

7 References

1. Heron, M. Deaths: Leading Causes for 2017. 77.
2. What to know about sudden death in young people. *Mayo Clinic* https://www.mayoclinic.org/diseases-conditions/sudden-cardiac-arrest/in-depth/sudden-death/art-20047571.
3. Rakowski, H. & Li, Q. Predicting Long-Term Outcomes in Asymptomatic or Minimally Symptomatic Patients With HCM. *JACC Cardiovasc. Imaging* **7**, 37–39 (2014).
4. Hypertrophic cardiomyopathy - Symptoms and causes. *Mayo Clinic* https://www.mayoclinic.org/diseases-conditions/hypertrophic-cardiomyopathy/symptoms-causes/syc-20350198.
5. Woo, A. *et al.* Mutations of the β myosin heavy chain gene in hypertrophic cardiomyopathy: critical functional sites determine prognosis. *Heart* **89**, 1179–1185 (2003).
6. Finer, J., Simmons, R. & Spudich, J. Single myosin molecule mechanics: piconewton forces and nanometre steps. *Nature* **368**, 113–119 (1994).
7. Murphy, C. T., Rock, R. S. & Spudich, J. A. A myosin II mutation uncouples ATPase activity from motility and shortens step size. *Nat. Cell Biol.* **3**, 311–315 (2001).
8. Cooper, G. M. Actin, Myosin, and Cell Movement. *Cell Mol. Approach 2nd Ed.* (2000).
9. How Fluorescence Microscopy Works - US. https://www.thermofisher.com/us/en/home/life-science/cell-analysis/cell-analysis-learning-center/molecular-probes-school-of-fluorescence/imaging-

basics/fundamentals-of-fluorescence-microscopy/how-fluorescence-microscopy-works.html.

10. *The 2018 Physics Nobel Prize: What ARE Optical Tweezers?*
11. Woerdemann, M. Introduction to Optical Trapping. in *Structured Light Fields* 5–26 (Springer Berlin Heidelberg, 2012). doi:10.1007/978-3-642-29323-8_2.
12. Kitamura, K., Tokunaga, M., Iwane, A. H. & Yanagida, T. A single myosin head moves along an actin ®lament with regular steps of 5.3 nanometres. **397**, 8 (1999).
13. Cardiac Muscle Tissue | Interactive Anatomy Guide. *Innerbody* https://www.innerbody.com/image_musc01/musc71.html.
14. Physiology of cardiac conduction and contractility | McMaster Pathophysiology Review. http://www.pathophys.org/physiology-of-cardiac-conduction-and-contractility/.
15. 19.2 Cardiac Muscle and Electrical Activity – Anatomy and Physiology. https://opentextbc.ca/anatomyandphysiology/chapter/19-2-cardiac-muscle-and-electrical-activity/.
16. Sugiura, S. *et al.* Comparison of Unitary Displacements and Forces Between 2 Cardiac Myosin Isoforms by the Optical Trap Technique: Molecular Basis for Cardiac Adaptation. *Circ. Res.* **82**, 1029–1034 (1998).
17. Biga, L. M. *et al.* 10.2 Skeletal Muscle. in *Anatomy & Physiology* (OpenStax/Oregon State University).
18. Davies, H. Electrical signals of the heart. https://www.ebme.co.uk/articles/clinical-engineering/electrical-signals-of-the-heart.

19. Cooper, G. M. Structure and Organization of Actin Filaments. *Cell Mol. Approach 2nd Ed.* (2000).
20. Figure 2. Array treadmilling providing cell front protrusion as modeled... *ResearchGate* https://www.researchgate.net/figure/Array-treadmilling-providing-cell-front-protrusion-as-modeled-in-the-reported-work-Actin_fig2_49785506.
21. Uyeda, T. Q. P., Kron, S. J. & Spudich'f, J. A. Estimation From Slow Sliding Movement of Actin Over Low Densities of Heavy Meromyosin. 12.
22. Cytoskeleton | Leaders in Pharmaceutical Business Intelligence (LPBI) Group. https://pharmaceuticalintelligence.com/tag/cytoskeleton/.
23. Hartman, M. A. & Spudich, J. A. The myosin superfamily at a glance. *J. Cell Sci.* **125**, 1627–1632 (2012).
24. Fenix, A. M. & Burnette, D. T. Assembly of myosin II filament arrays: Network Contraction versus Expansion. *Cytoskeleton* **75**, 545–549 (2018).
25. BIOL2060: Cell Biology. http://www.mun.ca/biology/desmid/brian/BIOL2060/BIOL2060-16/CB16.html.
26. Muscles. http://www2.nau.edu/gaud/bio301/content/musc.htm.
27. Dziedzic, J. M., Bjorkholm, J. E. & Chu, S. Observation of a single-beam gradient force optical trap for dielectric particles. 3.
28. Schirber, M. Focus: Nobel Prize—Lasers as Tools. *Physics* **11**, (2018).
29. Shaevitz, J. W. A Practical Guide to Optical Trapping. 19.
30. Optical tweezers. *Wikipedia* (2020).
31. Neuman, K. C. & Block, S. M. Optical trapping. *Rev. Sci. Instrum.* **75**, 2787–2809 (2004).

32. *Microscopy: Introduction to Fluorescence Microscopy (Nico Stuurman)*.
33. Dobrucki, J. W. Fluorescence Microscopy. in *Fluorescence Microscopy* (ed. Kubitscheck, U.) 97–142 (Wiley-VCH Verlag GmbH & Co. KGaA, 2013). doi:10.1002/9783527671595.ch3.
34. *Encyclopedia of Optical Engineering*. (Taylor & Francis, 2011). doi:10.1081/E-EOE.
35. Granite. Jablonski Diagram | What is it? *Edinburgh Instruments* https://www.edinst.com/blog/jablonski-diagram/.
36. CF®488A Dye. *Biotium* https://biotium.com/technology/cf-dyes/cf488a-dye/.
37. Rhodamine Phalloidin. https://www.thermofisher.com/order/catalog/product/R415#/R415.
38. Alexa Fluor™ 488 NHS Ester (Succinimidyl Ester). http://www.thermofisher.com/order/catalog/product/A20000.
39. Conjugation and color (video) | Spectroscopy. *Khan Academy* https://www.khanacademy.org/science/organic-chemistry/spectroscopy-jay/uv-vis-spectroscopy/v/conjugation-and-color-1.
40. Photons. http://electron6.phys.utk.edu/phys250/modules/module%201/photons.htm.
41. A12379 Documents & Support | Thermo Fisher Scientific. https://www.thermofisher.com/search/results?query=A12379&sort=relevancy&refinementAction=true&persona=DocSupport.
42. ImageJ. https://imagej.nih.gov/ij/.
43. Download. https://imagej.nih.gov/ij/download.html.

44. Walcott, S., Warshaw, D. M. & Debold, E. P. Mechanical Coupling between Myosin Molecules Causes Differences between Ensemble and Single-Molecule Measurements. *Biophys. J.* **103**, 501–510 (2012).
45. What is Hooke's Law? https://phys.org/news/2015-02-law.html.
46. *Microscopy: Optical Traps: Building and Calibrating (Carlos Bustamante)*.
47. Elert, G. Simple Harmonic Oscillator. *The Physics Hypertextbook* https://physics.info/sho/.
48. Corner Frequency - an overview | ScienceDirect Topics. https://www.sciencedirect.com/topics/engineering/corner-frequency.
49. Derivation of Hooke's Law from the Work-Energy Theorem - YouTube. https://www.youtube.com/watch?v=AM8IJaaU2rs.